Carboxylate-functionalized sugarcane bagasse as an effective and renewable adsorbent to remove methylene blue

Su-nv Wang, Ping Li, Jing-jing Gu, Hao Liang and Jin-hua Wu

ABSTRACT

This study prepared a carboxylate-functionalized sugarcane bagasse (CF-SCB) from sugarcane bagasse (SCB) via a simple and low-toxicity chemical modification to enhance its capacity for adsorbing methylene blue (MB) from aqueous solutions. The success of chemical modification was confirmed by scanning electron microscopy (SEM), Fourier transform infrared spectroscopy (FTIR), the pore area and porosity, and zeta potential measurement analysis. The adsorption capacity of CF-SCB was investigated at different pHs, ionic strengths, temperatures, contact times and initial dye concentrations. Equilibrium data were best described by the Langmuir isotherm model, and the maximum monolayer adsorption capacity of CF-SCB (296.74 mg g^{-1}) was greatly improved compared with SCB (77.16 mg g^{-1}) at 30 °C. The thermodynamic study indicated that MB adsorption onto CF-SCB was a spontaneous, endothermic and entropy increased process. Adsorption kinetics followed a pseudo-second-order mode, and the adsorption mechanism was based on electrostatic interactions. The reusability study showed that CF-SCB had reasonably good reuse potential. All the results suggested that CF-SCB has high potential to be used as an effective and renewable adsorbent for MB removal from wastewater.

Key words | adsorption, carboxylate-functionalized, methylene blue, sugarcane bagasse

Su-nv Wang
Ping Li (corresponding author)
Jin-hua Wu
The Key Laboratory of Pollution Control and Ecosystem Restoration in Industry Clusters, State Key Laboratory of Pulp and Paper Engineering, Ministry of Education; School of Environment and Energy,
South China University of Technology,
Guangzhou 510006,
China
E-mail: *pli@scut.edu.cn*

Jing-jing Gu
Hao Liang
Water Purification Institute of Logistics Department of Guangzhou Military Region,
Guangzhou 510500,
China

INTRODUCTION

Industrial wastewaters, such as dyestuffs, tannery, textiles, paper and plastics wastewaters, contain various synthetic dyes (Wei *et al.* 2015). Among those different types of synthetic dyes, azo dyes are the most widely used. It is estimated that up to 70% of synthetic dyes are from the azo dye group (-N = N-). Azo dyes generally are hard to degrade because of their photolysis resistance and oxidation resistance. They can reduce visibility in water bodies and restrain photosynthetic activity of aquatic plants (Akrout *et al.* 2015). In addition, azo dyes and their sub-products may be carcinogenic and mutagenic, and when released into natural waters, they can seriously damage the environment. Consequently, the presence of azo dyes has become an urgent problem in wastewater.

Many techniques have been developed to remove dyes from wastewaters, including flocculation/coagulation, aerobic and anaerobic processes, adsorption, electrochemical reaction and advanced oxidation. Among these methods, adsorption is recognized as a superior approach due to its high efficiency in removing various pollutants and convenient procedure (Rafatullah *et al.* 2010). Nevertheless, conventional adsorbents, such as activated carbon, zeolite, clay, and polymer, have various limitations and disadvantages. In addition to being non-selective and ineffective in adsorbing azo dyes, some of these materials have a high capital. Therefore, in the past few years, adsorbents prepared from natural biomass materials have obtained much attention. Various adsorbents based on agricultural wastes and by-products have been studied and applied to remove synthetic dyes from aqueous solutions (Gokce & Aktas 2014; Vakili *et al.* 2014; Peydayesh & Rahbar-Kelishami 2015). In most cases, these agricultural wastes and by-products are used as adsorbents without any chemical modification. Thus, the adsorption ability of these original materials is weak for lack of functional groups. Chemical modification can introduce functionality

doi: 10.2166/wst.2018.113

to these solid materials, and increasing their adsorption capacity and efficiency (Rafatullah *et al.* 2010; Gokce & Aktas 2014; Yahya *et al.* 2015). Therefore, chemical modification is widely used to enhance the adsorption capacity and efficiency of these biomass materials.

Sugarcane bagasse (SCB) is a promising agricultural by-product because of its low-cost and renewable property. In addition, a large amount of SCB is available in the world, making it an attractive option to collect solid biomass material. The composition of SCB is 40–50% of cellulose, 25–30% of hemicelluloses, and 20–25% of lignins (Guimaraes Gusmao *et al.* 2013). All of these components have numerous hydroxyl groups that can be used as reactive sites to produce new adsorbent materials with specific properties. Researchers have examined various surface chemical modification methods for biomass materials. However, use of organic solvents such as pyridine, N,N′-dimethylacetamide, N,N′-dimethylformamide, and dimethyl sulfoxide, compromises the viability of the chemical modification process due to the high cost of the organic solvents and their toxicity (Guimaraes Gusmao *et al.* 2012, 2013; Vakili *et al.* 2014). The solvent-free mechanochemistry routes and ultrasound and microwave radiation cleaner routes have been reported to have low efficiency to introduce carboxyl functional groups (Melo *et al.* 2011; Kalidhasan *et al.* 2012).

As a result, this study aimed to prepare carboxylate-functionalized sugarcane bagasse (CF-SCB) via a simple and low-toxic procedure using monochloroacetic acid as etherifying agent. CF-SCB was characterized by SEM, FTIR, the pore area and porosity, and zeta potential measurements. For the adsorption experiments, MB was chosen since the target pollutants is the most commonly used cationic azo dyes and has serious negative impacts on environments (Akrout *et al.* 2015). Batch adsorption of CF-SCB removal of MB was studied at different pHs, ionic strengths, temperatures, contact times and initial dye concentrations. Finally, the studies of adsorption isotherms, adsorption thermodynamics, and adsorption kinetics were carried out to understand the underlying adsorption mechanism.

MATERIALS AND METHODS

Materials

Sugarcane bagasse was collected from a sugar factory at LiuZhou, GuangXi, China. Methylene blue (MB, C.I. 52030, chemical formula $C_{16}H_{18}N_3OS$, λ_{max} 667 nm), monochloroacetic acid, hydrochloric acid (HCl), sodium hydrate (NaOH), ethanol, and other reagents were all A.R. grade. These reagents were purchased from Tianjin Damao (China) and used without further purification.

Preparation of CF-SCB

The collected sugarcane bagasse was broken into small pieces and subsequently dried at 70 °C in an oven for 12 h, then it was grounded to powder by milling with crusher. The powder was sieved in a two-sieve system (20 and 60 meshes). The fraction from 20 to 60 mesh was collected and washed with tap water to eliminate residual sugars, and then separated by filtration and dried at 70 °C in an oven as original sugarcane bagasse (SCB). Carboxymethylation of the sugarcane bagasse fiber sample was carried out according to Williamson's ether synthesis with minor modification (Tijsen *et al.* 2001; Pushpamalar *et al.* 2006). Briefly, the original SCB with 100 mL of solution containing 80% of ethanol in a 250 ml glass bottle. Subsequently, an aliquot of NaOH (22.2 mL, 20%) was added to this solution, followed by monochloroacetic acid (10.75 g). The mixture was then allowed to react in a shaking incubator at 80 °C for 3 h under constant stirring (120 rpm). After reaction termination, the modified material was separated by filtration, washed with 80% ethanol, until the pH was stable at 7.0, and then dried at 70 °C in an oven for 6 h to obtain carboxylate-functionalized sugarcane bagasse (CF-SCB). Figure 1(a) illustrates the synthesis path and the reaction mechanism for CF-SCB adsorbent preparation.

Characterization methods

The morphological features and surface characteristics of adsorbent materials were examined by scanning microscopy (SEM, Merlin, Zeiss, DE). The pore area and pore structure were determined by the mercury intrusion method (AutoPore IV 9500, Mike, USA). The zeta potentials of adsorbent materials were determined using a Zeta potentiometer (Zetasizer Nano ZS, Malvern, UK). In this method, aqueous solutions with pH values from 2.0 to 10.0 were prepared using 0.1 M HCl and 0.1 M NaOH. The prepared solution (100.0 mL) with different initial pH was added to each 250 mL Erlenmeyer flasks containing 0.05 g of samples. Then, zeta potentials was measured after shaking for 24 h. The Fourier transform infrared spectrometer (FTIR, Nicolet 6700, Thermo Fisher Scientific, USA) was used to identify the main characteristic bands of adsorbent materials. The samples were recorded by the KBr pellet technique in the wave number range from 400 to 4,000 cm^{-1}.

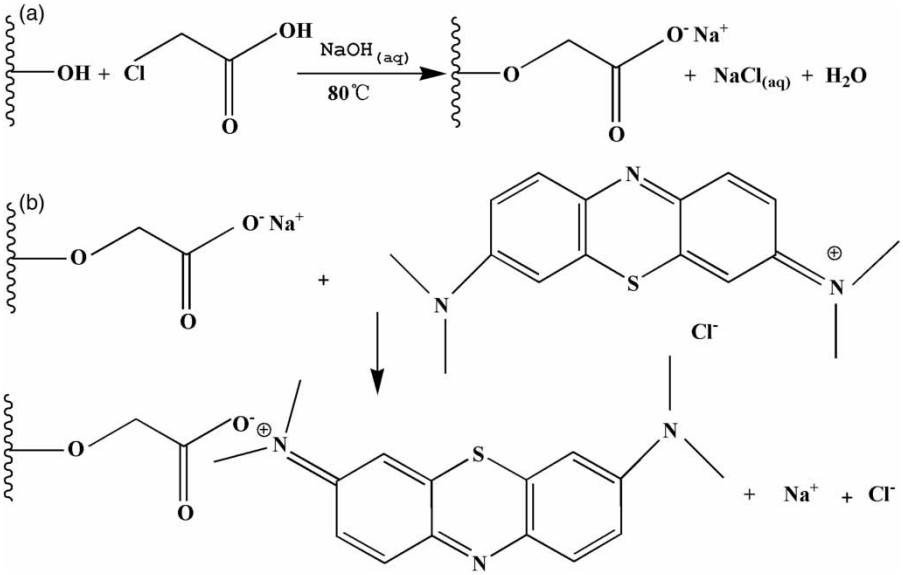

Figure 1 | (a) The synthesis path and the reaction mechanism to prepare CF-SCB adsorbent and (b) mechanism of MB adsorption onto CF-SCB.

Batch adsorption experiments

Adsorption experiments were conducted in a batch mode, MB solutions with target concentrations (0–800 mg/L) were prepared using distilled water. Then, 100 mL of MB at a known concentration was added to 250 mL Erlenmeyer flasks, adjusted to the required pH value (2.0–10.0), and placed in an oscillating constant temperature bath shaker (ZQWY-200G). When the temperature of the dye solutions reached the preset temperature (20–50 °C), accurately weighed absorbent material (1 g L^{-1}) was added into the MB solutions. After the Erlenmeyer flasks were sealed, the speed of the shaker was set at 120 rpm. At certain intervals (0.25–12 h), samples were taken from the solution and filtered (pore size 0.45 μm). And the concentration of MB in the filtrate was determined by a UV-visible spectrophotometer (UV2300) at 667 nm immediately. In the series of adsorption experiments, the pH of each solution was adjusted by adding HCl or NaOH (0.1 M).

Data analysis

In batch experiments, the adsorption capability of the absorbent for MB, q_e (mg g^{-1}), was calculated according to the following Equation (1):

$$q_e = \frac{(C_0 - C_e) \cdot V}{m} \tag{1}$$

where q_e (mg g^{-1}) is the amount of the MB adsorbed on the absorbent; C_0 and C_e (mg L^{-1}) are MB concentrations at initial and equilibrium states, respectively; V (L) is the solution volume; and m (g) is the mass of the adsorbent.

The isotherms experimental data have been fitted with three classical isotherm equations, i.e., Langmuir, Freundlich and Temkin (Guimaraes Gusmao *et al.* 2012) isotherms models.

The linear form of the Langmuir equation is (Equation (2)):

$$\frac{C_e}{q_e} = \frac{C_e}{q_L} + \frac{1}{k_L \cdot q_L} \tag{2}$$

The linear form of the Freundlich equation is (Equation (3)):

$$\lg q_e = \lg k_F + \frac{\lg C_e}{n} \tag{3}$$

The linear form of the Temkin equation is (Equation (4)):

$$q_e = A + b \ln C_e \tag{4}$$

where q_L (mg L^{-1}) is the theoretical saturated adsorption capacity; and k_L (L mg^{-1}) is the affinity parameter; k_F is the Freundlich isotherm constant; and 1/n is the heterogeneity factor; A (mg g^{-1}) is an equilibrium constant corresponding to the maximum energy of binding; and the constant b is related to the heat of adsorption.

For adsorption thermodynamic, the thermodynamic parameters values, Gibbs free energy change (ΔG, kJ mol^{-1}), enthalpy change (ΔH, kJ mol^{-1}) and entropy change (ΔS,

J mol^{-1} K^{-1}), were calculated using Equations (5) and (6):

$$\Delta G = -RT \ln K_C \tag{5}$$

$$\ln K_C = \frac{\Delta S}{R} - \frac{\Delta H}{RT} \tag{6}$$

where R (8.314 J mol^{-1} K^{-1}) is the ideal gas constant; T (K) is the solution temperature; and the distribution constant $K_c = q_e/C_e$. ΔH and ΔS were obtained by using the slope and intercept of plots of lnK_c versus 1/T.

For the kinetic experiment, dye solutions were taken at the particular time intervals. The amounts of CF-SCB adsorbed at a desired time t, q_t (mg g^{-1}), was calculated with Equation (7):

$$q_t = \frac{(C_t - C_0)V}{m} \tag{7}$$

where C_t (mg L^{-1}) is the MB concentrations in aqueous solution at a certain time t (h).

The kinetic data were analyzed by pseudo-first-order, pseudo-second-order, and Elovich kinetic models (Crini & Badot 2008).

The pseudo-first-order kinetic equation is (Equation (8)):

$$\frac{1}{q_t} = \frac{k_1}{q_e \cdot t} + \frac{1}{q_e} \tag{8}$$

The pseudo-second-order kinetic equation is (Equation (9)):

$$\frac{t}{q_t} = \frac{1}{k_2 \cdot q_e^2} + \frac{t}{q_e} \tag{9}$$

The Elovich equation is (Equation (10)):

$$q_t = \beta \cdot \ln(\alpha\beta) + \beta \cdot \ln t \tag{10}$$

Relative deviation, Δq (%), was used to measure the applicability of different kinetic models. The expression of Δq is shown in Equation (11):

$$\Delta q = \left| \frac{q_{e,\exp} - q_e}{q_e} \right| \times 100\% \tag{11}$$

where q_e (mg g^{-1}) is the adsorption capacity at equilibrium; k_1 (h) and k_2 (g mg^{-1} h^{-1}) are the pseudo-first-order and the pseudo-second-order rate constants, respectively; α (mg g^{-1} h^{-1}) is the initial adsorption rate, β is the initial adsorption rate; $q_{e,\exp}$ is experimental adsorption capacity at equilibrium.

RESULTS AND DISCUSSION

Characterization

Figure 2 shows the SEM micrographs of SCB and CF-SCB. The SCB sample had a smooth and fine morphological appearance with regular fibrous shapes in addition to a few powder fragments on the surface. After the modification, the CF-SCB adsorbent showed a bulged, clustered and rough surface, but kept the fiber texture shape well. This suggested that a chemical reaction occurred on the surface of the bagasse, and CF-SCB adsorbent is insoluble in aqueous solution (Wu *et al.* 2012).

Figure 3 shows the FTIR spectra for SCB and CF-SCB. As can be noticed, the wide peak at approximately 3,410 cm^{-1} was attributed to the stretching vibrations of -OH functional group (Reddy *et al.* 2017). The peak observed at 1,400 cm^{-1} was attributed to the C = C–H groups in plane bending (Sharma & Kaur 2011). The peak at 1,630 cm^{-1} represented skeletal vibrations of the benzene ring. After chemical modification, it can be obviously seen that two new peaks appeared at 1,740 and 1,240 cm^{-1}. The former band was assigned to the C = O stretch vibration of the carbonyl group (Qian & Chen 2014). The latter band was assigned to the stretch vibration of C-O associated with the carboxyl group (Lin *et al.* 2017), indicating that carboxyl groups were introduced to the surface of the sugarcane bagasse. The intensities of the peaks at 3,410 cm^{-1} became weaker, demonstrating that the introduction of carboxyl groups consumed hydroxyl groups in the etherification reaction (Xu *et al.* 2016). In addition, a strong band at 1,050 cm^{-1} which was indicative of C-O-C, became stronger after modification, also demonstrating that the etherification reaction happened on the surface of the SCB. The band at 2,940 cm^{-1} corresponding to asymmetric stretching of -CH_2 arose in the surface of CF-SCB. In summary, the FTIR characterization results proved that carboxyl groups have been successfully grafted onto SCB by the etherification reaction with monochloroacetic acid.

Table 1 shows the porous structure parameters of SCB and CF-SCB. Compared with SCB, the average pore diameter increased by 7.34 μm. The residual organic matter such as lignin could be solubilized and washed away by NaOH and monochloroacetic acid during treatment,

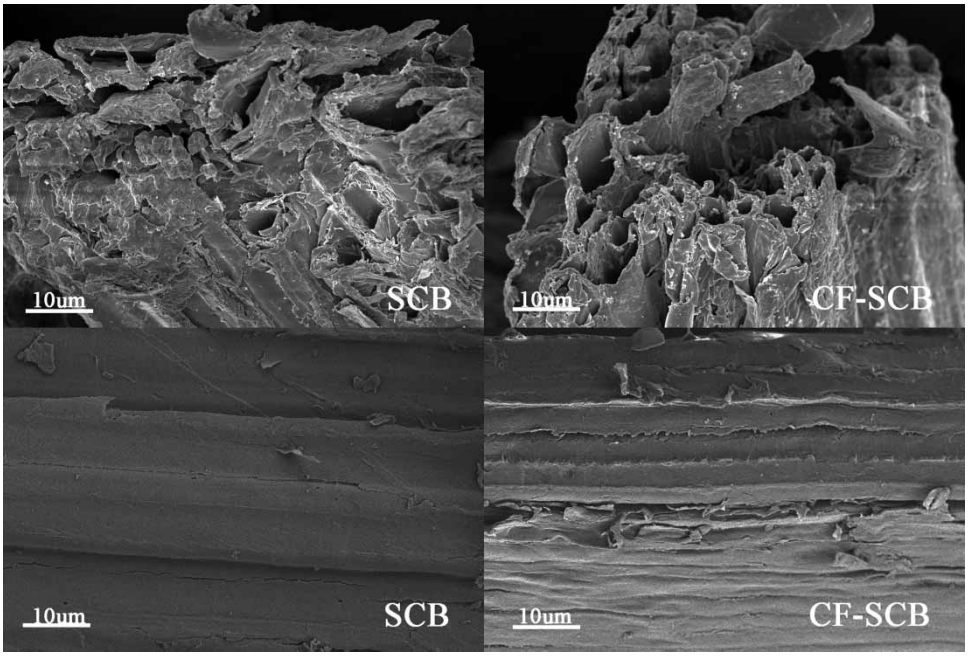

Figure 2 | SEM micrographs of SCB and CF-SCB.

which could account for the increase in the average pore size (Kong *et al.* 2014; Xu *et al.* 2016), and the average pore diameter (Figure S1, available with the online version of this paper) showed that the main pores of SCB and CF-SCB are of macroporous porosity. The total pore area decreased by 0.63 $m^2 g^{-1}$, which was consistent with previous studies (Chen *et al.* 2003; Xu *et al.* 2016). Total intrusion volume and total porosity of bagasse exhibited almost no change before and after modification, which showed that chemical modification did not change the number of pores and pore volume. It should be noted that the adsorption capacity of MB onto CF-SCB did not decrease but was significantly improved after chemical modification. These results indicated that the functional groups play a more important role than pore area and pore volume in the MB adsorption process.

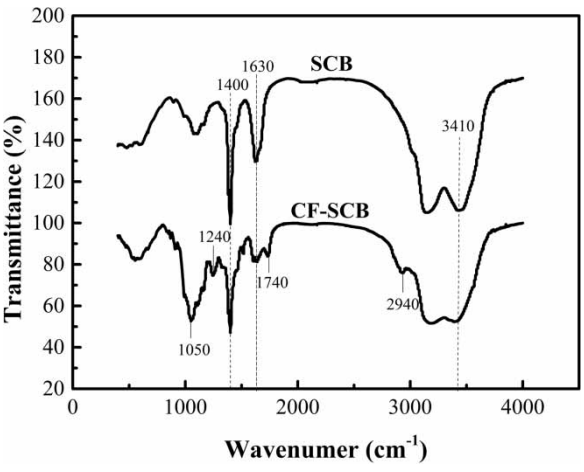

Figure 3 | FTIR spectra of SCB and CF-SCB.

Effect of initial pH

The effects of initial pH on MB adsorption onto the adsorbent were studied using 100 mg L^{-1} of MB aqueous solutions with a fixed adsorbent dose (1 g L^{-1}) at 30 °C. Figure 4 shows the results of MB adsorption and zeta potential variation onto CF-SCB and SCB from pH 2.0 to pH 10.0. It could be interpreted that CF-SCB has more negative charge on the surface because of the carboxyl group, resulting in the higher adsorption capacity of MB than SCB at the same pH. The adsorption capacity of SCB was nearly independent of pH and always at a low level. For CF-SCB, the adsorption capacity was negligible at pH = 2. Since the presence of excessive hydronium (H_3O^+) ions can compete with MB for the adsorption sites at a lower pH, the carboxyl groups

Table 1 | The porous structure parameters of SCB and CF-SCB

Sample	Total pore area ($m^2 g^{-1}$)	Average pore diameter μm	Total intrusion volume (mL g^{-1})	Total porosity %
SCB	1.35	10.69	3.61	82.13
CF-SCB	0.72	18.33	3.29	82.30

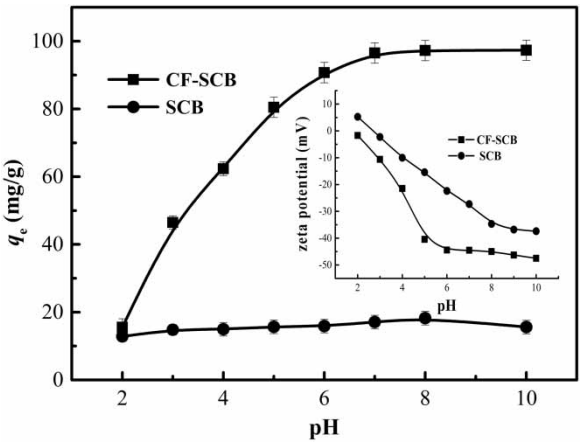

Figure 4 | The adsorption of MB and the zeta potential onto CF-SCB and SCB at different pHs.

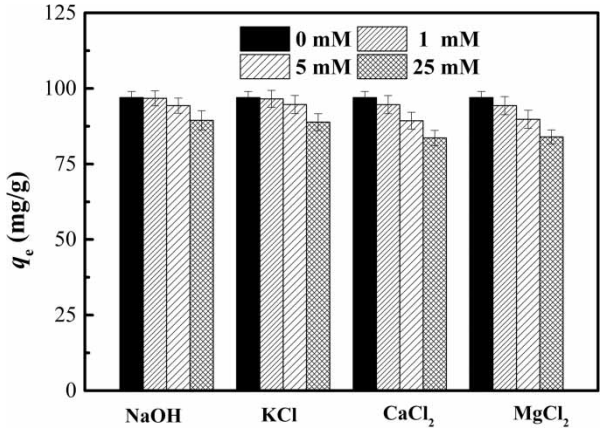

Figure 5 | Effect of ionic strengths on the adsorption of MB onto CF-SCB.

of CF-SCB were protonated (Lin *et al.* 2017), and MB adsorption onto CF-SCB was unfavorable. When the initial pH increased from 2.0 to 7.0, the adsorption capacity of CF-SCB for MB increased rapidly from 15.56 to 96.52 mg g^{-1}. This was because, with the increase in pH, the carboxyl groups in the CF-SCB adsorbent were deprotonated and had more negative charges in their surface to attract cationic dye MB, and showed higher adsorption capacity. Between pH 7.0 and 10.0, the adsorption capacity of MB was stable at around 97.00 mg g^{-1}, the appropriate pH interval for adsorption of MB on CF-SCB was from 7.0 to 10.0, and the optimum pH was 8.0. Similar studies reported on wood (Janos *et al.* 2009), tea waste (Uddin *et al.* 2009), and waste wheat straw (Lin *et al.* 2017) to remove MB. This observation leads to the conclusion that the adsorption mechanism is based on electrostatic interactions between the negatively surface charged CF-SCB and the positively charged MB.

Effect of ionic strength

The effects of ionic strength were investigated using 100 mg L^{-1} MB aqueous solutions with a fixed adsorbent dose (1 g L^{-1}) at pH7.0 and 30 °C. Figure 5 illustrates MB adsorption onto CF-SCB at different ionic strengths. The MB adsorption amount decreased slightly when the ionic strength (NaCl, KCl, $CaCl_2$ or $MgCl_2$) increased from 0 to 25 mM. By contrast, at the identical concentration, the divalent electrolyte ($CaCl_2$ and $MgCl_2$) had a more pronounced effect on the adsorption of MB than the univalent electrolyte (NaCl and KCl). When the concentration of Na^+, K^+, Ca^{2+} and Mg^{2+} was increased from 0 to 25 mM, the adsorption amount of MB changed from 97.02 to 89.46, 88.87, 83.64 and 83.98 mg g^{-1}, respectively. The decrease in adsorption capacity was due to the competition of salt ions with the positively charged MB for the same negatively charged adsorption sites on the surface of CF-SCB. Besides, Ca^{2+} and Mg^{2+} more positively charged can occupy more adsorption sites than Na^+ and K^+. Similar adsorption behavior for the effect of salt ionic strengths has been reported in previous studies (Wang *et al.* 2010; Xu *et al.* 2016). This result confirmed the involvement of electrostatic attraction in the MB adsorption onto CF-SCB, which was consistent with the analysis of the effect of pH above.

Adsorption isotherms

The adsorption isotherm experiments of MB on CF-SCB at different temperatures (20 °C, 30 °C, 40 °C, and 50 °C) as well as the control experiment using SCB at 30 °C were performed at a pH around 7.0, and are shown in Figure 6. When the initial concentration of MB was low, adsorption capacity was low because some adsorption sites in the surface of the adsorbents had not been occupied efficiently. With the increase in concentration, the adsorption quantity increased duo to adsorption sites being full. Comparing the adsorption quantity of MB on CF-SCB and SCB, it can be clearly seen that the maximum adsorption capacity of MB onto CF-SCB was about four times higher than that on SCB at 30 °C, indicating that carboxyl groups on SCB greatly enhanced the adsorption capacity. In addition, the adsorption capacity of CF-SCB increased slightly with temperature.

For further study of the adsorption phenomenon, the collected isotherms experimental data have been fitted with the Langmuir, Freundlich and Temkin models. According to their linear equations (Equations (2)–(4)), the

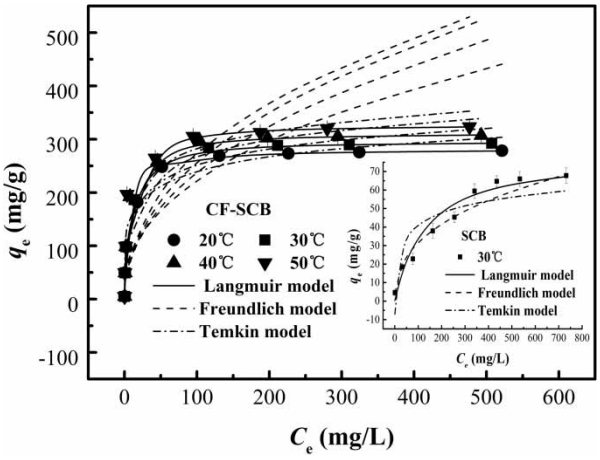

Figure 6 | Isotherms of MB adsorption onto CF-SCB at various temperatures (20 °C, 30 °C, 40 °C and 50 °C) and the comparative isotherm of SCB at 30 °C.

predicted curves were depicted and shown in Figure 6. The simulated parameters are listed in Table 2. Based on the coefficient of determination (R^2) of the linear form (Figure S2, available with the online version of this paper) for the three models, the R^2 values of the Langmuir model were much closer to 1.0 than those of the other two models at different temperatures. According to Figure 6, the maximum MB adsorption estimated from the Langmuir model was very close to the experimental value. These results indicated that the adsorption behavior of MB onto CF-SCB could be better described by the Langmuir model and MB was in monolayer coverage on the surface of CF-SCB. Moreover, according to the Langmuir model, the maximum adsorption capacities for MB of sugarcane bagasse increased from 77.16 to 296.74 (mg g^{-1}) at 30 °C after the carboxylate-functionalized modification.

Adsorption thermodynamic

In practical applications, the energy changes in an adsorption process can be predicted according to thermodynamic parameters values. Table 3 indicates the thermodynamic parameters of MB adsorption onto CF-SCB calculated by by Equations (5) and (6). The ΔG values of the adsorption at 293, 303, 313 and 323 K, are −9.21, −9.67, −9.83 and −10.86 kJ mol^{-1}, respectively. All the negative values of ΔG confirmed that the adsorption reaction is spontaneous in this experiment. With the increase in temperature, the value of ΔG became more negative, which indicated that MB adsorption onto CF-SCB was more thermodynamically favorable at high temperature. The adsorption ΔH value for MB on CF-SCB was 6.89 kJ mol^{-1}, confirming the adsorption process is an endothermic reaction. In addition, the positive value of ΔS indicated that randomness increases at the solid/solution interface during the adsorption (Bestani *et al.* 2008; Sharma & Kaur 2011).

Adsorption kinetics

The adsorption kinetics study was carried out at different contact times (0.25–12 h) with a fixed adsorbent quantity (1 g L^{-1}) in 100 mL of MB solution (100 mg L^{-1}) at 30 °C, and pH 7.0. Figure 7 shows the adsorption kinetics of MB onto CF-SCB. Of note, the adsorption of MB onto CF-SCB was fast in the first 1 h for abundantly available adsorption sites, and after that, it became slower close to the equilibrium. At the time of 3 h, it should be noted that about 95% of the total MB was removed, and the equilibrium times was 9 h.

To further investigate the adsorption rate and find the interaction mechanism of MB adsorption onto CF-SCB,

Table 3 | Adsorption thermodynamic model constants

T (K)	q_e (mg g^{-1})	lnk_c	ΔG (kJ mol^{-1})	ΔH (kJ mol^{-1})	ΔS (J mol^{-1} K^{-1})
293	97.77	3.78	−9.21	6.89	54.77
303	97.89	3.84	−9.67		
313	98.02	3.90	−9.83		
323	98.28	4.06	−10.86		

The values of q_e were obtained from Figure 6.

Table 2 | Isotherm parameters for the adsorption of MB onto CF-SCB and SCB

		Langmuir			Freundlich			Temkin		
Samples	Temperature (°C)	k_L (L mg^{-1})	q_L (mg g^{-1})	R^2	k_F (mg g^{-1})	n	R^2	A (mg g^{-1})	b	R^2
CF-SCB	20	0.147	281.69	0.995	35.92	2.495	0.725	75.31	36.510	0.976
	30	0.138	296.74	0.999	33.22	2.315	0.757	70.11	40.263	0.974
	40	0.140	312.50	0.997	35.26	2.298	0.732	74.66	42.644	0.965
	50	0.145	327.87	0.998	42.18	2.437	0.685	90.14	42.568	0.951
SCB	30	0.001	77.16	0.896	5.66	2.619	0.976	1.91	8.995	0.736

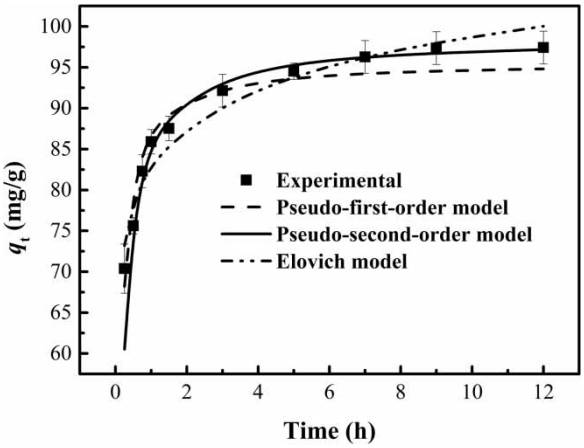

Figure 7 | Adsorption kinetics of MB onto CF-SCB fitted to the pseudo-first-order, pseudo-second-order models, and the Elovich model.

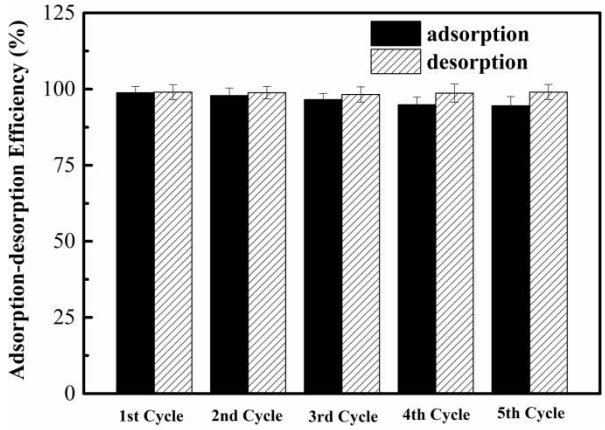

Figure 8 | Adsorption and desorption efficiency of CF-SCB.

the pseudo-first-order, pseudo-second-order, and the Elovich kinetic models were employed to analyze the experimental data (Figure S3, available with the online version of this paper). Table 4 shows the simulated kinetic parameters for each model. Based on the coefficient of determination (R^2), it was found that the adsorption kinetics of CF-SCB were fitted better to the pseudo-second-order kinetic model ($R^2 = 0.998$). Moreover, the value of q_e (98.83 mg g^{-1}) calculated from the pseudo-second-order model was in good agreement with the experimental value (97.84 mg g^{-1}) in Figure 7, and the relative deviation (Δq) was about 1.00%, and less than the relative deviation (2.29%) of the pseudo-first-order kinetic model. Thus, adsorption phenomenon of the MB onto CF-SCB followed the pseudo-second-order model during all periods of adsorption, supporting the model presupposition that the adsorption is controlled by a chemical adsorption involving valent forces (Sun *et al.* 2013). In addition, the Elovich equation fitted the experimental data well ($R^2 = 0.942$),

Table 4 | Kinetic parameters of MB adsorption onto CF-SCB

Kinetics model	Parameters	CF-SCB (1 g L^{-1})
Pseudo-first order	q_e (mg g^{-1})	95.60
	k_1 (h^{-1})	0.100
	R^2	0.928
	Δq (%)	2.29
Pseudo-second order	q_e (mg g^{-1})	98.83
	k_2 (g mg^{-1} h^{-1})	0.064
	R^2	0.998
	Δq (%)	1.00
Elovich model	$\alpha \times 10^4$	2.239
	β	6.928
	R^2	0.942

indicating the existence of MB chemisorption onto CF-SCB (Crini & Badot 2008). These results were consistent with the effect of pH and ionic strength, that the adsorption mechanism of MB onto CF-SCB is based on electrostatic interactions. As a result, the chemisorption involving valent forces is between the carboxyl binding sites of CF-SCB and the positively charged MB (Yan *et al.* 2011; Silva Ferreira *et al.* 2015). Furthermore, Figure 1(b) shows the adsorption mechanism of MB onto CF-SCB.

Regeneration and reusability evaluation of CF-SCB

The reusability study of the adsorbent was performed by batch adsorption and desorption tests to evaluate the reuse potential of CF-SCB. For this, 100 mg L^{-1} of MB solution was used, and five cycles of adsorption and desorption were run. After each adsorption, the MB-loaded adsorbent was desorbed in 0.1 M HCl solution and washed with distilled water and saturated sodium bicarbonate. The acid solution containing desorbed MB was determined for the concentration of MB. Figure 8 shows the efficiency of the five adsorption–desorption cycles. At the end of each cycle, CF-SCB exhibited over 96% adsorption efficiency, and desorption efficiency was about 100%. In other words, over the five cycles, adsorption uptake decreased slightly, and desorption efficiency was fairly maintained. This result indicated that the regeneration and reuse efficiency of CF-SCB is reasonably good, and CF-SCB can be well reused.

CONCLUSIONS

This study confirmed that a simple and low-toxic procedure using monochloroacetic acid can be feasibly employed to

prepare CF-SCB. Chemical modification could significantly enhance the MB removal ability of sugarcane bagasse by increasing the adsorption sites on the surface due to the introduction of carboxyl functional groups. In addition, the underlying mechanism of MB adsorption onto CF-SCB involved the electrostatic interactions between the dye cations and negatively charged carboxyl groups on the surface of the CF-SCB. MB adsorption on CF-SCB was pH dependent and the appropriate pH interval was from 7.0 to 10.0, the optimum pH was 8.0. Ionic strength had a slight effect on the adsorption. The adsorption equilibrium was best fitted by the Langmuir isotherm model, and the maximum monolayer adsorption capacities of CF-SCB were found to be 281.69, 296.74, 312.50 and 327.87 mg g^{-1} at 20, 30, 40 and 50 °C, respectively. The results suggested the equilibrium adsorption of MB onto CF-SCB was about 4 times higher than that on SCB at 30 °C. Thermodynamic data indicated that the process of MB adsorption on CF-SCB is spontaneous, endothermic and entropy increased. The adsorption process was best described by the pseudo-second-order kinetic model and was controlled by a chemical process. The exhausted CF-SCB adsorbent could be effectively regenerated and maintained ideal removal ability to MB after multiple cycle adsorptions. In conclusion, the objective of providing a simple and low-toxicity procedure to prepare CF-SCB was successful in this study, and CF-SCB could be used as an effective and renewable adsorbent to remove azo dyes such as MB.

ACKNOWLEDGEMENTS

The authors acknowledge support from the Special fund project of science and technology development in Guangdong Province (2017B020247025), the Fundamental Research Funds for the Central Universities (2017ZD025), the Water Resource Science and Technology Innovation Program of Guangdong Province (2016-26), the State Key Laboratory of Pulp and Paper Engineering (201627), and the help from Dr Chi-qian Zhang of the University of Missouri in the United States during the modified process of this paper.

REFERENCES

Akrout, H., Jellali, S. & Bousselmi, L. 2015 Enhancement of methylene blue removal by anodic oxidation using BDD electrode combined with adsorption onto sawdust. *Comptes Rendus Chimie* **18** (1), 110–120.

Bestani, B., Benderdouche, N., Benstaali, B., Belhakem, M. & Addou, A. 2008 Methylene blue and iodine adsorption onto an activated desert plant. *Bioresource Technology* **99** (17), 8441–8444.

Chen, J. P., Wu, S. N. & Chong, K. H. 2003 Surface modification of a granular activated carbon by citric acid for enhancement of copper adsorption. *Carbon* **41** (10), 1979–1986.

Crini, G. & Badot, P. 2008 Application of chitosan, a natural aminopolysaccharide, for dye removal from aqueous solutions by adsorption processes using batch studies: a review of recent literature. *Progress in Polymer Science* **33** (4), 399–447.

Gokce, Y. & Aktas, Z. 2014 Nitric acid modification of activated carbon produced from waste tea and adsorption of methylene blue and phenol. *Applied Surface Science* **313**, 352–359.

Guimaraes Gusmao, K. A., Alves Gurgel, L. V., Sacramento Melo, T. M. & Gil, L. F. 2012 Application of succinylated sugarcane bagasse as adsorbent to remove methylene blue and gentian violet from aqueous solutions – kinetic and equilibrium studies. *Dyes and Pigments* **92** (3), 967–974.

Guimaraes Gusmao, K. A., Alves Gurgel, L. V., Sacramento Melo, T. M. & Gil, L. F. 2013 Adsorption studies of methylene blue and gentian violet on sugarcane bagasse modified with EDTA dianhydride (EDTAD) in aqueous solutions: kinetic and equilibrium aspects. *Journal of Environmental Management* **118**, 135–143.

Janos, P., Coskun, S., Pilarova, V. & Rejnek, J. 2009 Removal of basic (Methylene Blue) and acid (Egacid Orange) dyes from waters by sorption on chemically treated wood shavings. *Bioresource Technology* **100** (3), 1450–1453.

Kalidhasan, S., Gupta, P. A., Cholleti, V. R., Kumar, A. S. K., Rajesh, V. & Rajesh, N. 2012 Microwave assisted solvent free green preparation and physicochemical characterization of surfactant-anchored cellulose and its relevance toward the effective adsorption of chromium. *Journal of Colloid and Interface Science* **372**, 88–98.

Kong, L., Xiong, Y., Sun, L., Tian, S., Xu, X., Zhao, C., Luo, R., Yang, X., Shih, K. & Liu, H. 2014 Sorption performance and mechanism of a sludge-derived char as porous carbon-based hybrid adsorbent for benzene derivatives in aqueous solution. *Journal of Hazardous Materials* **274**, 205–211.

Lin, Q., Wang, K., Gao, M., Bai, Y., Chen, L. & Ma, H. 2017 Effectively removal of cationic and anionic dyes by pH-sensitive amphoteric adsorbent derived from agricultural waste-wheat straw. *Journal of the Taiwan Institute of Chemical Engineers* **76**, 65–72.

Melo, J. C. P., Silva Filho, E. C., Santana, S. A. A. & Airoldi, C. 2011 Synthesized cellulose/succinic anhydride as an ion exchanger. Calorimetry of divalent cations in aqueous suspension. *Thermochimica Acta* **524** (1–2), 29–34.

Peydayesh, M. & Rahbar-Kelishami, A. 2015 Adsorption of methylene blue onto Platanus orientalis leaf powder: kinetic, equilibrium and thermodynamic studies. *Journal of Industrial and Engineering Chemistry* **21**, 1014–1019.

Pushpamalar, V., Langford, S. J., Ahmad, M. & Lim, Y. Y. 2006 Optimization of reaction conditions for preparing carboxymethyl cellulose from sago waste. *Carbohydrate Polymers* **64** (2), 312–318.

Qian, L. & Chen, B. 2014 Interactions of aluminum with biochars and oxidized biochars: implications for the biochar aging process. *Journal of Agricultural and Food Chemistry* **62** (2), 373–380.

Rafatullah, M., Sulaiman, O., Hashim, R. & Ahmad, A. 2010 Adsorption of methylene blue on low-cost adsorbents: a review. *Journal of Hazardous Materials* **177** (1–3), 70–80.

Reddy, D. D., Ghosh, R. K., Bindu, J. P., Mahadevaswamy, M. & Murthy, T. G. K. 2017 Removal of methylene blue from aqueous system using tobacco stems biomass: kinetics, mechanism and single-stage adsorber design. *Environmental Progress & Sustainable Energy* **36** (4), 1005–1012.

Sharma, P. & Kaur, H. 2011 Sugarcane bagasse for the removal of erythrosin B and methylene blue from aqueous waste. *Applied Water Science* **1** (3–4), 135–145.

Silva Ferreira, B. C., Teodoro, F. S., Mageste, A. B., Gil, L. F., de Freitas, R. P. & Alves Gurgel, L. V. 2015 Application of a new carboxylate-functionalized sugarcane bagasse for adsorptive removal of crystal violet from aqueous solution: kinetic, equilibrium and thermodynamic studies. *Industrial Crops and Products* **65**, 521–534.

Sun, L., Wan, S. & Luo, W. 2013 Biochars prepared from anaerobic digestion residue, palm bark, and eucalyptus for adsorption of cationic methylene blue dye: characterization, equilibrium, and kinetic studies. *Bioresource Technology* **140**, 406–413.

Tijsen, C. J., Kolk, H. J., Stamhuis, E. J. & Beenackers, A. 2001 An experimental study on the carboxymethylation of granular potato starch in non-aqueous media. *Carbohydrate Polymers* **45** (3), 219–226.

Uddin, M. T., Islam, M. A., Mahmud, S. & Rukanuzzaman, M. 2009 Adsorptive removal of methylene blue by tea waste. *Journal of Hazardous Materials* **164** (1), 53–60.

Vakili, M., Rafatullah, M., Salamatinia, B., Abdullah, A. Z., Ibrahim, M. H., Tan, K. B., Gholami, Z. & Amouzgar, P. 2014 Application of chitosan and its derivatives as adsorbents for dye removal from water and wastewater: a review. *Carbohydrate Polymers* **113**, 115–130.

Wang, L., Zhang, J., Zhao, R., Li, C., Li, Y. & Zhang, C. 2010 Adsorption of basic dyes on activated carbon prepared from *Polygonum orientale* Linn: equilibrium, kinetic and thermodynamic studies. *Desalination* **254** (1–3), 68–74.

Wei, Y., Ding, A., Dong, L., Tang, Y., Yu, F. & Dong, X. 2015 Characterisation and coagulation performance of an inorganic coagulant-poly-magnesium-silicate-chloride in treatment of simulated dyeing wastewater. *Colloids and Surfaces A-Physicochemical and Engineering Aspects* **470**, 137–141.

Wu, Z., Cheng, Z. & Ma, W. 2012 Adsorption of Pb(II) from glucose solution on thiol-functionalized cellulosic biomass. *Bioresource Technology* **104**, 807–809.

Xu, Y., Liu, Y., Liu, S., Tan, X., Zeng, G., Zeng, W., Ding, Y., Cao, W. & Zheng, B. 2016 Enhanced adsorption of methylene blue by citric acid modification of biochar derived from water hyacinth (*Eichhornia crassipes*). *Environmental Science and Pollution Research* **23** (23), 23606–23618.

Yahya, M. A., Al-Qodah, Z. & Ngah, C. W. Z. 2015 Agricultural bio-waste materials as potential sustainable precursors used for activated carbon production: a review. *Renewable & Sustainable Energy Reviews* **46**, 218–235.

Yan, H., Zhang, W., Kan, X., Dong, L., Jiang, Z., Li, H., Yang, H. & Cheng, R. 2011 Sorption of methylene blue by carboxymethyl cellulose and reuse process in a secondary sorption. *Colloids and Surfaces A-Physicochemical and Engineering Aspects* **380** (1–3), 143–151.

First received 16 August 2017; accepted in revised form 26 February 2018. Available online 9 March 2018